

# Non-equilibrium electroweak baryogenesis at preheating after inflation

Juan García-Bellido

*Theoretical Physics, Blackett Laboratory, Imperial College, Prince Consort Road, London SW7 2BZ, U.K.*

Dmitri Grigoriev

*Institute for Nuclear Research of Russian Academy of Sciences, Moscow 117312, Russia*

Alexander Kusenko

*Department of Physics, University of California, Los Angeles CA 90095-1547, U.S.A.*

Mikhail Shaposhnikov

*Institute for Theoretical Physics, University of Lausanne, CH-1015 Lausanne, Switzerland*

(February 23, 1999)

We present a novel scenario for baryogenesis in a hybrid inflation model at the electroweak scale, in which the Standard Model Higgs field triggers the end of inflation. One of the conditions for successful baryogenesis, the departure from thermal equilibrium, is naturally achieved at the stage of preheating after inflation. The inflaton oscillations induce large occupation numbers for long-wavelength configurations of Higgs and gauge fields, which leads to a large rate of sphaleron transitions. We estimate this rate during the first stages of reheating and evaluate the amount of baryons produced due to a particular type of higher dimensional CP violating operator. The universe thermalizes through fermion interactions, at a temperature below critical,  $T_{\text{rh}} \lesssim 100$  GeV, preventing the wash-out of the produced baryon asymmetry. Numerical simulations in (1+1) dimensions support our theoretical analysis.

PACS numbers: 98.80.Cq Preprint IMPERIAL-TP-98/99-39, UCLA/99/TEP/7, hep-ph/9902449

## I. INTRODUCTION

One of the most appealing explanations for the baryon asymmetry of the universe utilizes the non-perturbative baryon-number-violating sphaleron interactions present in the electroweak model at high temperatures [1,2]. In addition to B, C and CP violating processes, a departure from thermal equilibrium is necessary for baryogenesis [3]. The usual scenario invokes a strongly first-order phase transition to drive the primordial plasma out of equilibrium and set the stage for baryogenesis [2]. This scenario presupposes that the universe was in thermal equilibrium before and after the electroweak phase transition, and far from it during the phase transition. However, there is no reason to believe that the universe was in thermal equilibrium before the electroweak symmetry breaking, nor that it went through a phase transition. According to the recent studies of reheating after inflation, the universe could have undergone a period of “preheating” [4], during which only certain modes are highly populated and the system remains very far from thermal equilibrium. Eventually, thermalization takes place via the fermionic interactions that break the coherence of the bosonic fields.

The absence of a usual thermal phase transition does not preclude electroweak baryogenesis. On the contrary, the highly non-equilibrium state [5] produced at “preheating” creates an environment in which a substantial

baryon asymmetry could be created. The sphaleron transitions, known to cause baryon number violation at high temperature, may also proceed in a system out of thermal equilibrium. In addition, the very non-equilibrium nature of preheating may facilitate the baryon number generation, as emphasized in Ref. [6] in the context of GUT baryogenesis. In this paper we discuss the possibility that the electroweak baryogenesis took place during the preheating era at the end of a period of electroweak-scale inflation.

We consider a hybrid model of inflation [7], in which the inflaton is a  $SU(2) \times U(1)$ -singlet and the ordinary Higgs doublet is the triggering field that ends inflation. Alternatively, one can view this process as one in which the inflaton coupling to the Higgs induces dynamical electroweak symmetry breaking, when the inflaton slow-rolls below a certain critical value. The necessary flatness of the inflaton potential can be supported by (softly broken) supersymmetry. The resonant decay of the low-energy inflaton can generate a high-density Higgs condensate characterized by a set of narrow spectral bands in momentum space with large occupation numbers. The system evolves towards equilibrium while slowly populating higher and higher momentum modes. The expansion of the universe at the electroweak scale is negligible compared to the mass scales involved, so the energy density is conserved, and the final reheating temperature  $T_{\text{rh}}$  is determined by the energy stored initially in the inflaton

field. We will find model parameters such that the final thermal state has a temperature below the electroweak scale,  $T_{\text{rh}} < T_c \sim 100$  GeV.

Sphalerons are large extended objects sensitive mainly to the infrared part of the spectrum. We will conjecture that the rate of sphaleron transitions at the non-equilibrium stage of preheating after inflation can be estimated as  $\Gamma_{\text{sph}} \sim \alpha_{\text{W}}^4 T_{\text{eff}}^4$ , where  $T_{\text{eff}}$  is some “effective” temperature associated with the long wavelength modes of the Higgs and gauge fields that have been populated during preheating.

Since  $T_{\text{rh}} < T_c$ , the baryon-violating processes, relatively frequent in the non-thermal condensate, are strongly suppressed as soon as the plasma thermalizes via the interaction with fermions. Therefore, the baryon asymmetry created at the end of preheating is not washed out. This is in contrast to the equilibrium electroweak baryogenesis, where the main constraint arises from the tendency for the baryon density to equilibrate back to zero during the slow cooling following the electroweak phase transition. Since the energy density at the electroweak scale is so low, the universe expansion is essentially irrelevant and does not affect the prediction for the baryon asymmetry.

The paper is organized as follows. In section II we discuss the hybrid inflationary model suitable for non-equilibrium electroweak baryogenesis. We estimate the sphaleron rates and produced baryon asymmetry in section III. As our estimates are based on a number of assumptions on complicated non-linear dynamics we perform a numerical analysis of two-dimensional gauge-Higgs system in section IV. Our analytical results are in good agreement with the numerical simulations presented in this section. We draw our conclusions in Section V.

## II. AN INFLATIONARY MODEL FOR THE ELECTROWEAK BARYOGENESIS DURING PREHEATING

Inflation is often associated with processes occurring at the very high energy scales, of order the Grand Unification Scale ( $\sim 10^{16}$  GeV), see Ref. [8]. However, this need not be the case. Low-scale inflation models have been considered [7,9,10]. One of the side benefits of lowering the inflation scale is avoiding the gravitino overproduction constraints. There are other particle-physics motivations for using the TeV scale, which is associated with supersymmetry breaking in a class of models [11]. We will propose a simple hybrid inflation model which satisfies the constraints from cosmic microwave background (CMB) anisotropies and large-scale structure, and at the same time contains the desired features for a successful reheating of the universe.

As described in the introduction, we want to construct a model with a reheating temperature which is below that of the electroweak scale, so that sphaleron processes

are suppressed after reheating. Such a model necessarily has a very low rate of expansion during inflation,  $H \sim \rho^{1/2}/M_P \approx 10^{-5}$  eV, which is many orders of magnitude smaller than the mass scales we will consider. This means that essentially all the energy density during inflation is converted into radiation in less than a Hubble time, *i.e.* before the universe has had a chance to expand significantly. This imposes a very strict constraint on the energy scale during inflation<sup>1</sup>. For example, if we want the universe to reheat to  $T_{\text{rh}} \lesssim 100$  GeV, we need a model of inflation with an energy density of order  $\rho_0^{1/4} \sim 200$  GeV. We will construct an example of such a model.

Hybrid inflation [7] is an ingenious model of inflation, in which the amplitude of CMB anisotropies is not necessarily related to the GUT scale physics [8]. The idea is very simple: instead of ending inflation via deviations from the slow-roll, it is the symmetry breaking by a scalar field coupled to the inflaton that triggers the end of inflation. The model can then satisfy the CMB constraints [12,13] and allow for the electroweak-scale inflation. We will assume that the symmetry breaking field is in fact the Standard Model Higgs field, and that the inflaton is an additional  $SU(2) \times U(1)$ -singlet scalar field. The model thus contains two fields, the inflaton  $\sigma$  with mass  $\tilde{m}$ , coupled, with coupling  $g$ , to the Higgs field  $H^\dagger H = \phi^2/2$ , with false vacuum energy  $V_0 = M^4/4\lambda$  and the vacuum expectation value  $\phi_0 = M/\sqrt{\lambda} \equiv v$ ,

$$V(\sigma, \phi) = \frac{\lambda}{4}(\phi^2 - v^2)^2 + \frac{1}{2}\tilde{m}^2\sigma^2 + \frac{1}{2}g^2\sigma^2\phi^2. \quad (1)$$

During inflation, the inflaton is large,  $\sigma \gg \sigma_c \equiv M/g$ , and the effective mass of  $\phi$  is, therefore, large and positive. As a consequence, the Higgs field is fixed at  $\phi = 0$  and does not contribute to the metric perturbations that gave rise to the observed CMB anisotropies. As the inflaton field slowly rolls in the effective potential  $V(\sigma) = V_0 + \tilde{m}^2\sigma^2/2$ , it will generate the perturbations observed by COBE on large scales [12]. Eventually, the inflaton reaches  $\sigma = \sigma_c$ , where the Higgs has an effective zero mass, and at this point the quantum fluctuations of the Higgs field trigger the electroweak symmetry breaking and inflation ends. The number of e-folds of inflation required to solve the horizon and flatness problems is given by

$$N_e \simeq 34 + \ln\left(\frac{T_{\text{rh}}}{100\text{GeV}}\right). \quad (2)$$

The fluctuations seen by COBE on the largest scales could have arisen in this model,  $N_e \simeq 34$  e-folds before

---

<sup>1</sup>One can avoid such constraints by coupling the inflaton to some additional hidden-sector fields that do not contribute to the reheating of the observable universe. Then the potential energy density during inflation can be significantly larger than  $\rho \sim (200 \text{ GeV})^4$ .

the end of inflation. The observed amplitude and tilt of CMB temperature anisotropies [12,13],  $\delta T/T \simeq 2 \times 10^{-5}$ , and  $n - 1 \lesssim 0.1$ , imposes the following constraints on the model parameters [14]:

$$g \left( \frac{v}{M_{\text{Pl}}} \right)^3 \frac{M^2}{\tilde{m}^2} \simeq 1.2 \times 10^{-5}, \quad (3)$$

$$n - 1 = \frac{1}{\pi} \left( \frac{M_{\text{Pl}}}{v} \right)^2 \frac{\tilde{m}^2}{M^2} < 0.1. \quad (4)$$

For example, for  $v = 246$  GeV (the electroweak symmetry breaking vacuum expectation value),  $\lambda \simeq 1$ , and  $g \simeq 0.1$ , we find  $\tilde{m} \simeq 2 \times 10^{-12}$  eV, and it turns out that the spectrum is essentially scale-invariant,  $n - 1 \simeq 5 \times 10^{-14}$ . These parameters give a negligible rate of expansion during inflation,  $H \simeq 7 \times 10^{-6}$  eV, and a reheating temperature  $T_{\text{rh}} \simeq 70$  GeV. The small mass for the inflaton field along the flat direction can be naturally obtained in models of gauge-mediated supersymmetry breaking at the scale  $\sim 10^3$  TeV with Planck-scale suppressed radiative corrections,  $\tilde{m} \sim (10^3 \text{ TeV})^3 / M_{\text{Pl}}^2 \sim 10^{-11}$  eV.<sup>2</sup> However, the relevant masses for us here are those in the true vacuum, where the Higgs has a mass  $m_{\text{H}} = \sqrt{2\lambda} v \simeq 350$  GeV, and the inflaton field a mass  $m = gv \simeq 25$  GeV. Such field, a singlet with respect to the standard model (SM) gauge group, could be detected at future colliders because of its large coupling to the Higgs field [16].

Some comments are in order. The consideration carried out below is qualitatively applicable also to a more complicated theory than the minimal SM. Let us take the minimal supersymmetric standard model (MSSM) with an additional singlet field, the inflaton  $\sigma$ , as an example. There are three SU(2) invariant couplings of the inflaton to the Higgs doublets  $H_1$  and  $H_2$ :  $g_{11}\sigma^2\epsilon_{\alpha\beta}H_1^\alpha H_1^\beta$ ,  $g_{22}\sigma^2\epsilon_{\alpha\beta}H_2^\alpha H_2^\beta$ , and  $g_{12}\sigma^2\epsilon_{\alpha\beta}H_1^\alpha H_2^\beta$ . The Higgs mass matrix of the MSSM has the eigenvalues that range from the lightest,  $\sim 100$  GeV, to the heaviest, roughly, 500 GeV [16]. In general, the inflaton-Higgs interaction is not diagonal in the basis that diagonalizes the Higgs mass matrix in the broken-symmetry vacuum. In fact, the entire Higgs mass matrix is important in determining the conditions for parametric resonance. We will leave the analysis of multiple Higgs degrees of freedom for future work because it is too complicated and is not necessary to illustrate the main idea.

### A. Preheating in hybrid inflation

To study the process of parametric resonance after the end of inflation in this model, let us recall some of the main features of preheating in hybrid inflation [17].

<sup>2</sup>These small masses also seem to be necessary for inflation in theories with large internal dimensions, see Ref. [15].

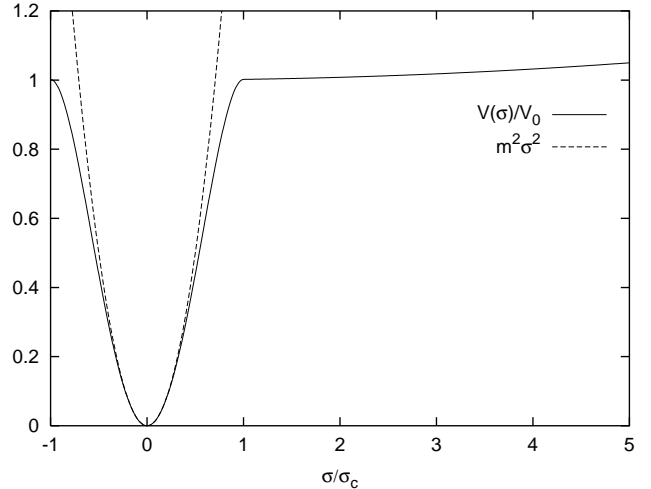


FIG. 1. The projected effective potential  $V(\sigma)/V_0$ , for the inflaton field  $\sigma/\sigma_c$  after the end of inflation. The dashed line corresponds to the  $m^2\sigma^2$  approximation around the minimum of the inflaton potential. Due to the shape of the potential at large  $\sigma$ , initial large-amplitude oscillations of the field  $\sigma$  are not exactly harmonic.

In hybrid models, after the end of inflation, the two fields  $\sigma$  and  $\phi$  start to oscillate around the absolute minimum of the potential,  $\sigma = 0$  and  $\phi = v$ , with frequencies that are much greater than the rate of expansion. Other bosonic and fermionic fields coupled to these may be parametrically amplified until the backreaction occurs and further rescattering drives the system to thermal equilibrium. Initially, rescattering of the long-wavelength modes among themselves drives them to local thermal equilibrium, while only a very small fraction of the short-wavelength modes are excited. The spectral density evolves slowly towards the higher and higher momenta [18,19]. Eventually, thermalization should occur through a process that breaks the coherence of the bosonic modes, e.g. through the decay of the Higgs or gauge fields into fermions. Such a process is very fast in the absence of the expansion of the universe. What prevented the universe from reheating immediately after inflation in chaotic models was the fact that the rate of expansion in those models was much larger than the decay rate of the inflaton, and particles did not interact with each other until the rate of expansion dropped below the decay rate. In our case, the opposite is true: the rate of expansion  $H \sim 10^{-5}$  eV is much smaller than the typical gauge field decay rate into fermions, and the universe thermalizes quickly. Since the masses are much greater than the rate of expansion, many oscillations (of order  $10^{15}$ ) occur in one Hubble time [17]. It is, therefore, possible to approximate the particle production by that in a flat Minkowski space-time [20].

The evolution equation for the Fourier component of the Higgs field that is subject to parametric resonance is approximately given by

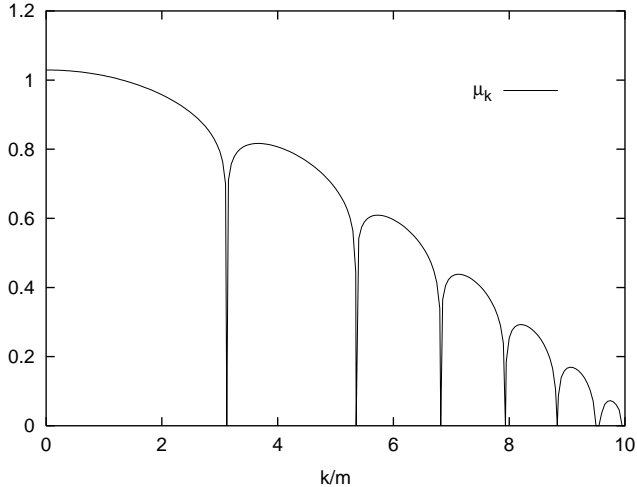


FIG. 2. The growth parameter  $\mu_k$  as a function of momenta  $k$ , in units of  $m$ , for a Higgs mass  $m_H = 350$  GeV. The occupation numbers for each mode  $k$  can be obtained from  $n_k = \exp(2\mu_k mt)/2$ .

$$\ddot{\phi}_k + [k^2 - M^2 + 3\lambda\langle\phi^2\rangle + g^2\sigma^2(t)]\phi_k = 0. \quad (5)$$

Note that this equation applies only in the case  $\lambda \gg g^2$ , where we have ignored the non-linear effect of the inflaton field  $\sigma$ , and in particular the cross-terms  $g^2\phi_k\sigma_k$ , which do not contribute significantly before backreaction [17]. We will only use this equation for qualitative arguments, since our quantitative results will be fully non-linear and non-perturbative, based on numerical simulations, see Section IV. As the inflaton oscillates around  $\sigma = 0$  with amplitude  $\Sigma = \sigma_c = M/g$  in the effective potential of Fig. 1, its coupling to the Higgs will induce the parametric resonance with a  $q$  parameter [21], characterizing the strength of the resonance, and given by

$$q \simeq \frac{g^2\Sigma^2}{4m^2} = \frac{\lambda}{4g^2} \gg 1. \quad (6)$$

Since we can neglect the rate of expansion, the amplitude of oscillations  $\Sigma$  does not decrease, and the resonance is extremely long-lived. For generic values of the couplings,  $g^2 \sim 10^{-2} - 10^{-3}$ , it is, in fact, a broad resonance,  $q \gg 1$ . Higgs particle production occurs at the instants when  $\sigma(t) = 0$ , and continues until backreaction becomes important, either for the inflaton oscillations ( $\langle\phi^2\rangle \simeq m^2/g^2$ ) [18,19,4] or for the effective Higgs mass ( $3\lambda\langle\phi^2\rangle \simeq M^2 - k_*^2 + 4m^2\sqrt{q}$ ) [4]. Which of the two effects back-reacts first depends on the coupling  $g$ . Here  $k_* = \sqrt{2}m q^{1/4}$  is the typical momentum of the resonance band. For  $g > 0.08$  backreaction on the inflaton mass occurs before the  $\lambda$ -term in (5) is relevant. We have chosen  $g = 0.1$  for definiteness, and computed the power spectrum of the Higgs field. For a smaller coupling  $g$ , the resonance spectrum would be different, but the qualitative behavior would be similar. In fact, it does not matter how many bands the parametric resonance populates because after rescattering all those bands smooth out and

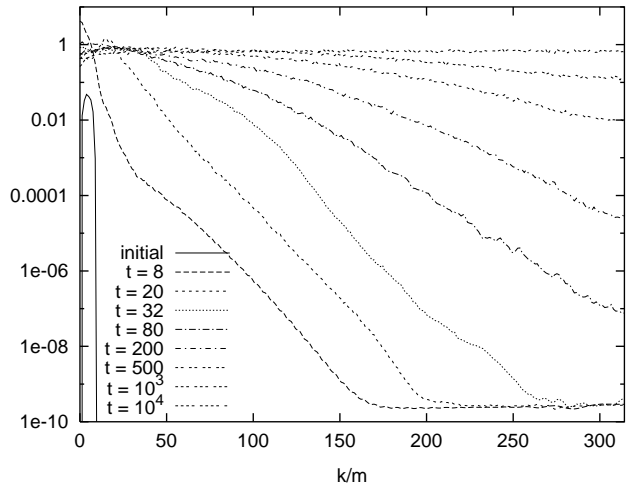


FIG. 3. The evolution of the Higgs spectrum  $n_k \omega_k$ , in units of  $v = 246$  GeV, from time 0 to  $10^4 v^{-1}$ , as a function of momentum,  $k/m$ . The initial spectrum is set by preheating, and contains a set of narrow bands (solid line). The subsequent evolution of the system leads to a redistribution of energy between different modes. Note how rapidly a “thermal” equidistribution is reached for the long-wavelength modes. However, the whole Higgs spectrum approaches thermalization already in the middle of resonance (see Fig. 4 below).

reach “thermalization” over a *finite* region in momentum space [18,19]. In Fig. 2 we show the growth parameter  $\mu_k$  as a function of  $k$ . The typical momentum contributing to the power spectrum,  $k^2|\phi_k|^2$ , is

$$k \sim k_*/2 = m q^{1/4}/\sqrt{2} \approx 2m, \quad (7)$$

where the growth factor has a large value,  $\mu_{\max} \simeq 0.9$ . This unusually large number is due to the fact that what drives the Higgs production in this model is not the usual parametric resonance from oscillations around the minimum of the potential [17], but the spinoidal instability responsible for the breaking of the electroweak symmetry. In the language of Mathieu equations [21], this corresponds to a large and negative  $A = (k^2 - M^2)/4m^2$  parameter, which induces large growth factors  $\mu$ . On the other hand, the occupation number of a given mode is determined from  $\mu_k$  as  $n_k \simeq \frac{1}{2} \exp(2\mu_k mt)$ . This means that, within a few oscillations, the Higgs field reaches a huge occupation number over a range of narrow bands in momentum space. Therefore, the Higgs fluctuations grow exponentially with time,

$$\langle\phi^2\rangle = \frac{1}{2\pi^2} \int dk k^2 \frac{n_k}{\omega_k} \simeq \frac{n_\phi(t)}{h\Sigma} \propto e^{2\mu mt}, \quad (8)$$

with  $\mu = \mu_{\text{eff}} \simeq 0.8$ . At backreaction, the Higgs expectation value is just of order its vacuum expectation value (VEV),  $\langle\phi^2\rangle \lesssim m^2/g^2 \simeq v^2$ , but continues to grow slightly during rescattering [18,19]. With our set of parameters, this happens at times  $t \sim \mathcal{O}(1)$  GeV $^{-1}$ .

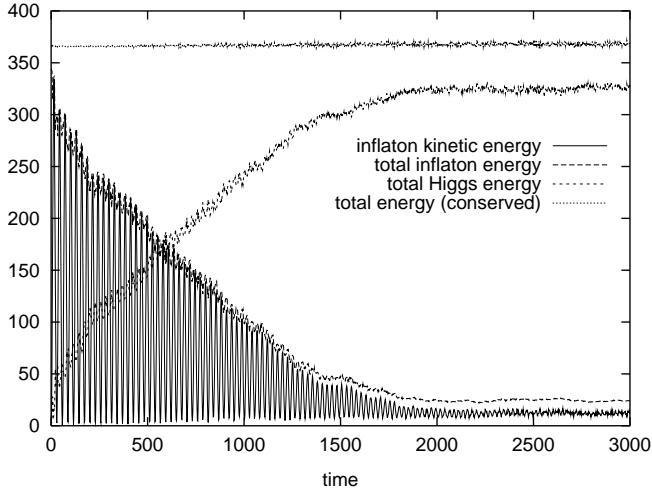


FIG. 4. The time evolution of the inflaton energy, the Higgs energy and the total energy. Note that the energy is measured in units of  $v$  and time in units of  $v^{-1}$ , see Ref. [22].

In Section IV of this paper we follow a numerical approach in (1+1) dimensions and computed the initial state from parametric resonance and subsequent stages like rescattering and backreaction directly through the real time evolution of the classical equations of motion for the bosonic modes with arbitrary  $k$ , with all the couplings between fields properly taken into account. This way, we have automatically included rescattering and thermalization in the evolution.

### B. Higgs coupling to W bosons

Soon after production, Higgs particles decay predominantly into  $W$  bosons with a branching ratio of order one, for  $m_H = 350$  GeV, and a decay rate  $\Gamma \sim 20$  GeV. One may ask whether the Higgs oscillations may induce a resonant production of gauge bosons. It turns out that the corresponding resonance is very narrow and insufficient ( $q_W m_H = g_W^2 \Phi^2 / 4m_H \simeq 0.3 \text{ GeV} \ll \Gamma$ , where  $g_W^2 = 4\pi\alpha_W$  is the SU(2) gauge coupling and  $\Phi \simeq v/10$  is the amplitude of the Higgs oscillations during the first resonance stage, see Fig. 9) for the coherent decay of the Higgs into gauge bosons. It is therefore appropriate to use perturbation theory to calculate the Higgs decay into the  $W$  bosons.

Since the rate of growth of the energy density of the Higgs field,

$$\rho_\phi = \frac{1}{2\pi^2} \int dk k^2 n_k \omega_k \simeq n_\phi(t) h \Sigma \propto e^{2\mu m t}, \quad (9)$$

is larger than its decay rate into  $W$  bosons, i.e.  $2\mu m \simeq 2\Gamma \sim 40$  GeV, we do not expect a significant depletion of the energy density of the Higgs field during preheating, while the energy density of the gauge bosons grows exponentially at the same rate,  $\rho_W \propto \exp(2\mu m t)$ . Therefore,

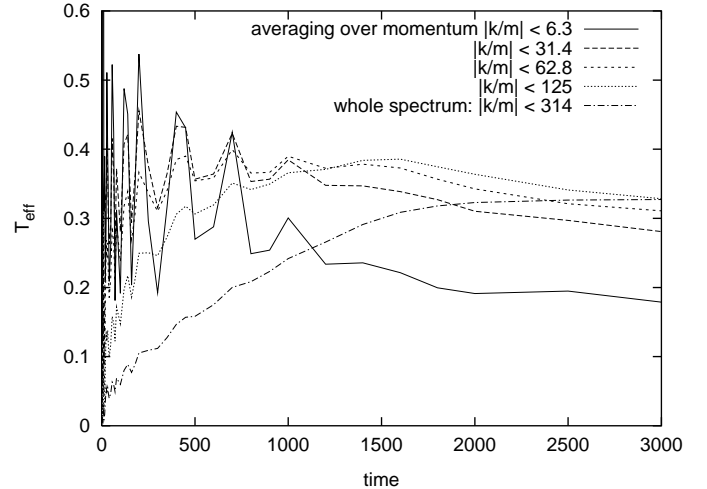


FIG. 5. The time evolution of the effective temperature, in units of  $v$ . We have averaged the Higgs power spectrum over different low-momentum regions, and we obtain several effective temperatures that show different time behavior.

soon after rescattering, most of the energy density is in the form of Higgs and gauge fields with essentially zero momentum. It is these long-wavelength gauge configurations that will play an important role in inducing the sphaleron transitions, and the subsequent baryon production.

One of the most fascinating properties of rescattering after preheating is that the long-wavelength part of the spectrum soon reaches some kind of local equilibrium [18,19], while the energy density is drained, through rescattering and excitations, into the higher frequency modes. Therefore, initially the low energy modes reach “thermalization” at a higher effective “temperature” [5], while the high energy modes remain unpopulated, and the system is still far from true thermal equilibrium:

$$n_k = \frac{1}{\exp(\omega_k/T) - 1} \approx \frac{T_{\text{eff}}}{\omega_k} \gg 1. \quad (10)$$

It is possible to estimate the effective “temperature”  $T_{\text{eff}}$  from the conservation of energy during preheating. The energy per (long wavelength) mode is  $n_k \omega_k \approx T_{\text{eff}}$ , or effectively equipartitioned. Since only the modes in the range  $0 < k \lesssim k_{\text{max}} \simeq 4k_* \sim 5m q^{1/4}$  are populated, we can integrate the energy density in Higgs and gauge fields,  $g_B = 1 + 3 \times 3 = 10$ , to give, in (3+1)-dimensions,

$$\begin{aligned} \rho_{\text{bosons}} &= g_B \int \frac{d^3k}{(2\pi)^3} n_k \omega_k \simeq \frac{g_B}{6\pi^2} T_{\text{eff}} k_{\text{max}}^3 \simeq \frac{\lambda v^4}{4}, \\ \frac{T_{\text{eff}}}{v} &\simeq \frac{6\pi^2 q^{1/4}}{125 g_B g} \propto g^{-1/2}, \end{aligned} \quad (11)$$

which gives  $T_{\text{eff}} \simeq 350$  GeV. We note that the effective temperature depends on the value of the coupling  $g$  as  $T_{\text{eff}}^4 \propto g^{-2}$ , as expected [4]. The temperature  $T_{\text{eff}}$  is higher than the final reheating temperature  $T_{\text{rh}}$ , which

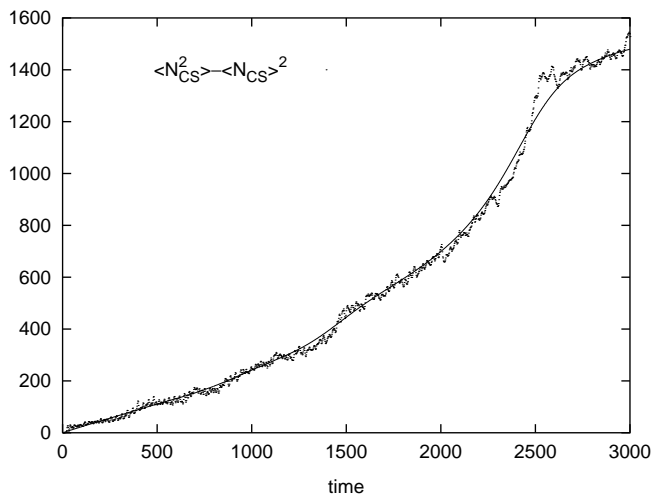


FIG. 6. The variance of the Chern-Simons number, i.e.  $\langle N_{CS}^2 \rangle - \langle N_{CS}(t) \rangle^2$ , as a function of time. The solid line is a result of smoothing out the measured values (dots).

is easy to understand, since preheating is a very efficient mechanism for populating just a few modes, into which a large fraction of the original inflaton energy density is put. This means that a few modes carry a large amount of energy as they come into partial equilibrium among themselves, and thus the effective “temperature” is high. However, when the system reaches a full thermal equilibrium, the same energy is distributed between all modes, which corresponds to a much lower temperature. In our example, thermalization of long-wavelength modes happens at a time scale  $t \sim \Gamma_w^{-1} \sim \mathcal{O}(1) \text{ GeV}^{-1}$ , where  $\Gamma_w \simeq 2 \text{ GeV}$  is the width of the vector boson.

This is the main reason why the out of equilibrium mechanism of preheating is so efficient in producing sphaleron transitions, since the rate of these transitions is greatly enhanced by the higher effective temperature. An alternative way of seeing this is by analogy with a diffusing plasma. The rescattering of Higgs and W bosons after preheating produces a diffusion which enhances over-the-barrier sphaleron transitions. It is fortunate that the description of this diffusion mechanism can be done with the use of an effective temperature, for which the rate of sphaleron transitions can be estimated analytically, by ignoring the higher momentum modes and the integration over hard thermal loops [23].

### III. BARYON ASYMMETRY OF THE UNIVERSE

It is well known that sphaleron transitions are mainly sensitive to the long-wavelength modes in a plasma. This is because the sphaleron size,  $(\alpha_w T_{\text{eff}})^{-1}$ , is much larger than the typical Compton wavelengths of particles in the plasma,  $(2k_*)^{-1} \simeq (5m)^{-1}$ . A simple argument then suggests that the rate of sphaleron transitions per unit time per unit volume should be of the order of the fourth power

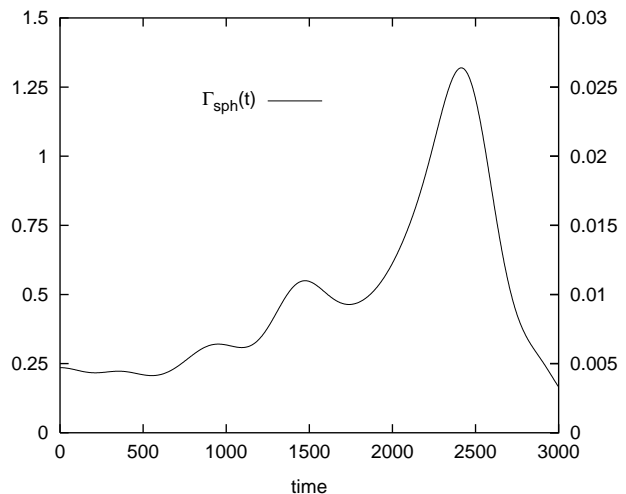


FIG. 7. The sphaleron transition rate  $\Gamma_{\text{sph}}(t)$  is proportional to the time derivative of the Chern-Simons variance (solid line on Fig. 6). The left scale measures the transitions per unit time per whole sample volume. The right scale measures the sphaleron transitions per unit time per unit volume. Note that because of high final equilibrium temperature the transitions aren’t vanishing after the resonance.

of the magnetic screening length in plasma [24,25].<sup>3</sup>

We, therefore, conjecture that the sphaleron transition rate during rescattering after preheating,  $\Gamma_{\text{sph}}$ , can be approximated by that of a system in thermal equilibrium at some temperature  $T_{\text{eff}}$  defined in the previous section:

$$\Gamma_{\text{sph}} \approx \alpha_w^4 T_{\text{eff}}^4. \quad (12)$$

In the Standard Model, baryon and lepton numbers are not conserved because of the non-perturbative processes that involve the chiral anomaly:

$$\partial_\mu j_B^\mu = \partial_\mu j_L^\mu = \frac{3g_w^2}{32\pi^2} F_{\mu\nu} \tilde{F}^{\mu\nu}. \quad (13)$$

Furthermore, the sphaleron configurations connect vacua with different Chern-Simons numbers,  $N_{CS}$ , and induce the corresponding changes in the baryon and lepton number,  $\Delta B = \Delta L = 3\Delta N_{CS}$ .

A baryon asymmetry can be generated by sphaleron transitions in the presence of C and CP violation. There

<sup>3</sup>In the symmetric phase of the electroweak theory and in thermal equilibrium at a temperature  $T$ , the typical momentum scale of sphaleron processes is  $\alpha_w T$  ( $\alpha_w \simeq 1/29$  is the weak gauge coupling) which is much smaller than average momentum of the particles in the plasma  $\sim T$ . It was argued in Refs. [26,23] that the higher momentum modes with typical scale greater than  $g_w T$  should slow down the sphaleron processes by an extra factor  $\alpha_w \log(1/\alpha_w)$ . During the first stages of reheating those high frequency modes are not populated and therefore should not be considered in our estimate.

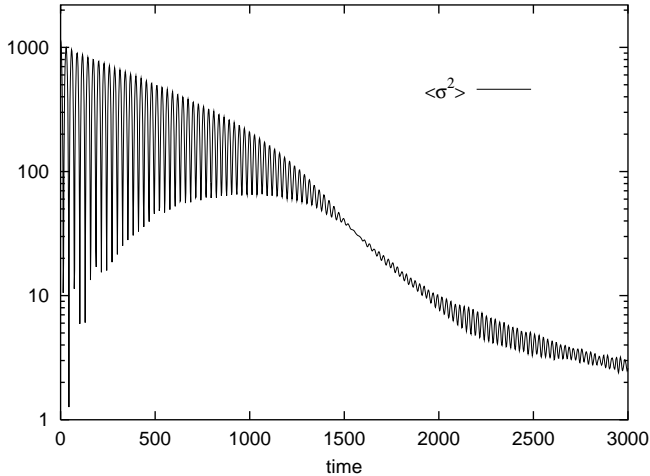


FIG. 8. The expectation value of  $\langle \sigma^2 \rangle$  in units of  $v^2$ , as a function of time.

are several possible sources of CP violation at the electroweak scale. The only one confirmed experimentally is due to Cabibbo-Kobayashi-Maskawa mixing of quarks that introduces some violation of CP, but it is probably too small to cause a sufficient baryon asymmetry. Various extensions of the Standard Model contain additional scalars (e.g. extra Higgs doublets, squarks, sleptons, *etc.*) with irremovable complex phases that lead to C and CP violation.

We are going to model the effects of CP violation in the effective field theory approach. Namely, we assume that, after all degrees of freedom except the gauge fields, the Higgs, and the inflaton are integrated out, the effective Lagrangian contains some non-renormalizable operators that break CP. The lowest, dimension-six operator of this sort is [27]

$$\mathcal{O} = \frac{\delta_{\text{CP}}}{M_{\text{new}}^2} \phi^\dagger \phi \frac{3g_w^2}{32\pi^2} F_{\mu\nu} \tilde{F}^{\mu\nu}. \quad (14)$$

The dimensionless parameter  $\delta_{\text{CP}}$  is an effective measure of CP violation, and  $M_{\text{new}}$  characterizes the scale at which the new physics, responsible for this effective CP violating operator, is important. Of course, other types of CP violating operators are possible although, qualitatively, they lead to the same picture.

Note that the operator (14) is CP-odd but does not violate C. Thus, in a pure bosonic theory non-equilibrium evolution can only produce parity-odd or CP-odd configurations, but no C asymmetry. For example, the Chern-Simons number can be produced, as it is C-even but P and CP-odd. C violation, necessary for baryogenesis, comes from ordinary gauge-fermion electroweak interactions that violate C and parity, but conserve CP. This manifests itself in the anomaly equation that relates baryon number (C-odd but P-even operator) to the Chern-Simons number (C = +1, P = -1). In other words, C violation in the bosonic sector of the theory is not re-

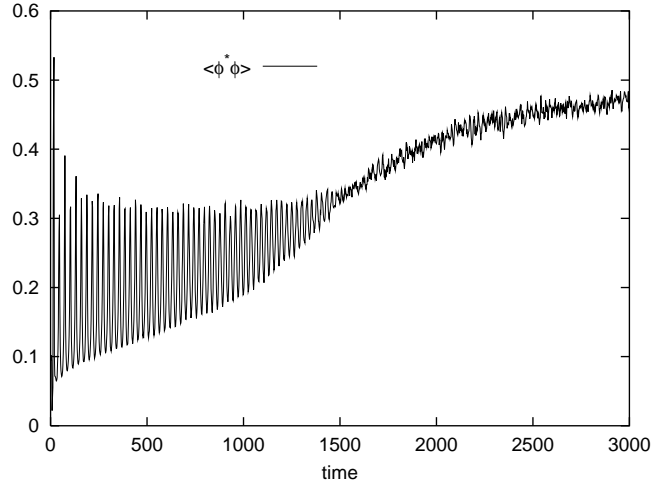


FIG. 9. The expectation value of  $\langle \phi^* \phi \rangle$ , in units of  $v^2$ , as a function of time. The variations in  $\langle \phi^* \phi \rangle$  give rise to a CP nonconserving chemical potential  $\mu_{\text{eff}}$ , which is the source of the baryon asymmetry.

quired as long as it appears in the fermionic sector, via the electroweak interactions.

If the scalar field is time-dependent, the vacua with different Chern-Simons numbers are not degenerate. This can be described quantitatively in terms of an effective chemical potential,  $\mu_{\text{eff}}$ , which introduces a bias between baryons and antibaryons,

$$\mu_{\text{eff}} \simeq \frac{\delta_{\text{CP}}}{M_{\text{new}}^2} \frac{d}{dt} \langle \phi^2 \rangle. \quad (15)$$

This equation follows from Eq. (14) by integration by parts. Although the system is very far from thermal equilibrium, we will assume that the evolution of the baryon number  $n_B$  can be described by a Boltzmann-like equation, where only the long-wavelength modes contribute,

$$\frac{dn_B}{dt} = \Gamma_{\text{sph}} \frac{\mu_{\text{eff}}}{T_{\text{eff}}} - \Gamma_B n_B, \quad (16)$$

where  $\Gamma_B = (39/2)\Gamma_{\text{sph}}/T_{\text{eff}}^3$ . The temperature  $T_{\text{eff}}$  decreases with time because of rescattering: the energy stored in the low-frequency modes is transferred to the high-momentum modes.

The rate  $\Gamma_B$ , even at high effective temperatures, is smaller than other typical scales in the problem. Indeed, for  $T_{\text{eff}} \sim 400$  GeV,  $\Gamma_B \sim 0.01$  GeV, which is small compared to the rate of the resonant growth of the Higgs condensate ( $2\mu m \sim 40$  GeV). It is also much smaller than the decay rate of the Higgs into W's and the rate of W decays into light fermions. Therefore, the last term in Eq. (16) never dominates during preheating and the final baryon asymmetry can be obtained by integrating

$$n_B = \int dt \Gamma_{\text{sph}}(t) \frac{\mu_{\text{eff}}(t)}{T_{\text{eff}}(t)} \simeq \Gamma_{\text{sph}} \frac{\delta_{\text{CP}}}{T_{\text{eff}}} \frac{\langle \phi^2 \rangle}{M_{\text{new}}^2}, \quad (17)$$

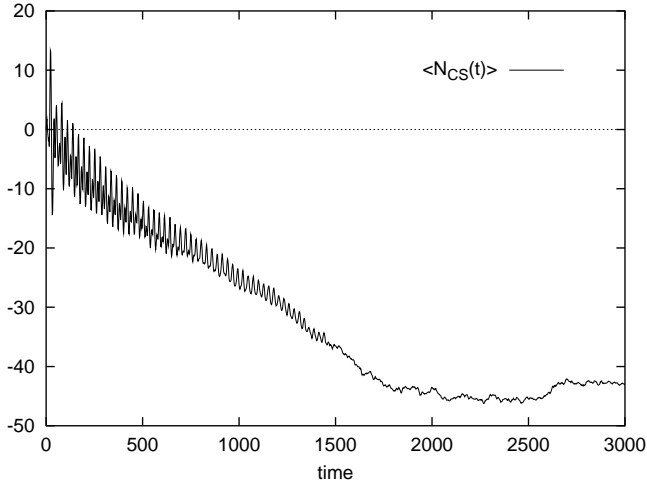


FIG. 10. The Chern-Simons number  $N_{CS}(t)$  averaged over 100 runs, for CP violating parameter  $\kappa = -1$ . Note that it settles at a large and negative  $N_{CS}$ , corresponding to large baryon production.

where all quantities are taken at the time of thermalization. This corresponds to a baryon asymmetry

$$\frac{n_B}{s} \simeq \frac{45\alpha_w^4 \delta_{CP}}{2\pi^2 g_*} \frac{\langle \phi^2 \rangle}{M_{\text{new}}^2} \left( \frac{T_{\text{eff}}}{T_{\text{rh}}} \right)^3, \quad (18)$$

where  $g_* = g_B + (7/8)g_F \sim 10^2$  is the number of effective degrees of freedom that contribute to the entropy density  $s$  at the electroweak scale. Taking  $\langle \phi^2 \rangle \simeq v^2 = (246 \text{ GeV})^2$ , the scale of new physics  $M_{\text{new}} \sim 1 \text{ TeV}$ , the coupling  $\alpha_w \simeq 1/29$ , the temperatures  $T_{\text{eff}} \simeq 350 \text{ GeV}$  and  $T_{\text{rh}} \simeq 70 \text{ GeV}$ , we find

$$\frac{n_B}{s} \simeq 3 \times 10^{-8} \delta_{CP} \frac{v^2}{M_{\text{new}}^2} \left( \frac{T_{\text{eff}}}{T_{\text{rh}}} \right)^3 \simeq 2 \times 10^{-7} \delta_{CP}, \quad (19)$$

consistent with observations for  $\delta_{CP} \simeq 10^{-3}$ , which is a reasonable value from the point of view of particle physics beyond the Standard Model. Therefore, baryogenesis at preheating can be very efficient in the presence of CP violation that comes from new physics at  $M_{\text{new}} \sim 1 \text{ TeV}$ .

#### IV. NUMERICAL SIMULATIONS IN (1+1) DIMENSIONS

The theoretical analysis presented above was based on the conjecture that the sphaleron transition rate can be described in terms of the effective “temperature”  $T_{\text{eff}}$  as in equation (12). This assumption is based on the reasoning given above and seems quite plausible. We have also verified the validity of such description in the (1+1)-dimensional numerical simulations.

For simplicity, we consider an Abelian Higgs model in (1+1) dimensions, which was successfully used before for studying physics relevant to baryogenesis [22,28,29]. The

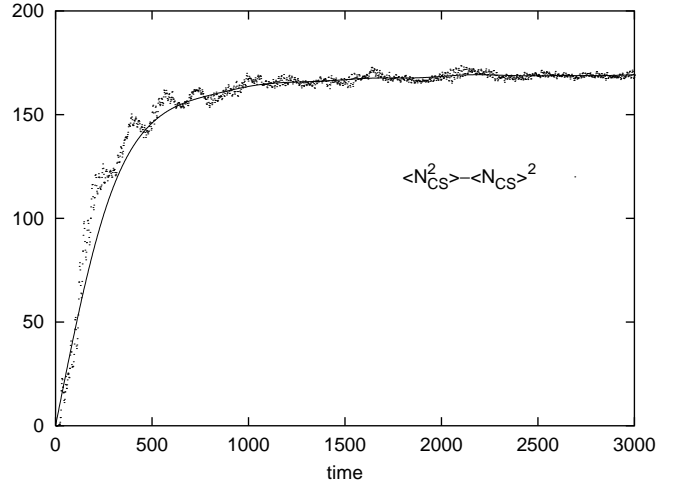


FIG. 11. The variance of the topological Chern-Simons number  $\langle N_{CS}^2 \rangle - \langle N_{CS} \rangle^2$  for a set of runs with total energy reduced by a factor of 4, as compared to runs in Figs. 3-10.

Lagrangian comprises two scalar fields and a U(1) gauge field:

$$\begin{aligned} \mathcal{L} = & -\frac{1}{4}F_{\mu\nu}^2 - \kappa|\phi|^2 \epsilon_{\mu\nu} F^{\mu\nu} \\ & + |D_\mu \phi|^2 - \lambda(|\phi|^2 - v^2/2)^2 \\ & + \frac{1}{2}(\partial_\mu \sigma)^2 - \frac{1}{2}\tilde{m}^2 \sigma^2 - g^2 \sigma^2 |\phi|^2, \end{aligned} \quad (20)$$

where  $D_\mu = \partial_\mu - ieA_\mu$ , with  $e$  the U(1) gauge coupling, and  $\epsilon_{\mu\nu}$  is the totally antisymmetric tensor in (1+1) dimensions. Here CP violation is induced via the  $\kappa \phi^* \phi \epsilon_{\mu\nu} F^{\mu\nu}$  term, which violates both C and CP. Furthermore, in (1+1) dimensions, the analogue of the chiral anomaly is the anomalous non-conservation of the gauge invariant fermionic current,  $j_F^\mu = \bar{\psi} \gamma^\mu \psi$ ,

$$\partial_\mu j_F^\mu = -\frac{e}{4\pi} \epsilon_{\mu\nu} F^{\mu\nu}, \quad (21)$$

which serves as a source of B violation.

The corresponding equations of motion are:

$$\begin{aligned} \partial_\nu F^{\mu\nu} + 2\kappa \epsilon^{\mu\nu} \partial_\nu |\phi|^2 &= e j_\phi^\mu, \\ D^2 \phi + 2\lambda \phi (|\phi|^2 - v^2/2) + g^2 \sigma^2 \phi &= -\kappa \phi \epsilon_{\mu\nu} F^{\mu\nu}, \\ \partial_\mu \partial^\mu \sigma + \tilde{m}^2 \sigma + 2g^2 |\phi|^2 \sigma &= 0, \end{aligned} \quad (22)$$

where  $j_\phi^\mu = i(\phi^* \partial^\mu \phi - \phi \partial^\mu \phi^*)$  is the charged current of the Higgs field.

The numerical simulations track the real time evolution of the classical field configurations. The initial conditions are set by preheating as a set of narrow bands in the Higgs power spectrum (Fig. 3). The real-time evolution leads to a gradual redistribution of energy between different modes, including the inflaton field  $\sigma$  itself. Note that the Higgs field takes a very long time to reach its VEV, see Fig. 9, due to the presence of the CP violating term in

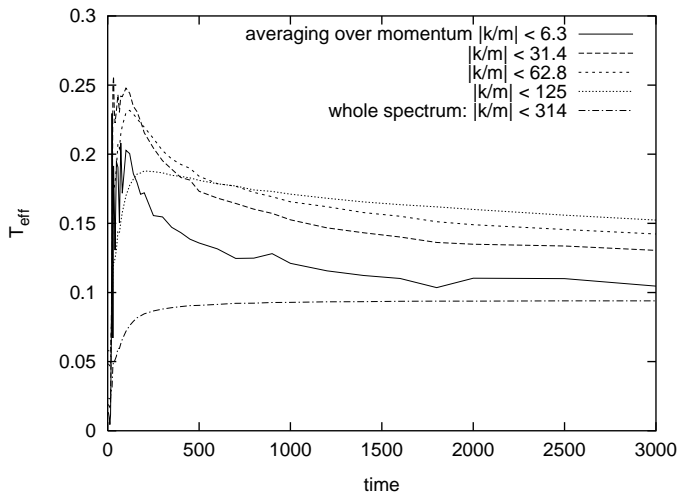


FIG. 12. The time evolution of effective temperature  $T_{\text{eff}}$  in units of  $v$ , for the reduced-energy runs. Note the smoother rise and decline of the effective temperature with time.

Eq. (22), which leads to the production of baryon number before equilibrium. In fact, the full thermalization of the system should take a very long time [19,30], while some other processes (e.g. interaction with fermions from the decay of gauge fields and/or Higgs) will induce thermalization via decoherence long before that. Thus, although it is technically possible to reach complete thermalization of the whole system including the inflaton, our simulations are necessarily limited to the vector and Higgs decay time scale, of order of 50 inflaton oscillations, as in Fig. 4.

### A. The sphaleron transition rate and the effective temperature

As expected, the resonant inflaton decay quickly leads to a population of the long-wavelength modes of the Higgs field, see Fig. 3. This happens after only a few oscillations of the inflaton. At this point the long-wavelength modes contain a very large fraction of the total energy, and that leads to a noticeable increase in  $T_{\text{eff}}$  at the beginning of the resonance, see Fig. 5.

The sphaleron transitions immediately set in. We monitor them both by calculating the Chern-Simons number,  $N_{\text{CS}} = \int A_1 dx^1$  in the temporal gauge  $A_0 \equiv 0$ , and also by keeping track of the U(1) winding number of Higgs field. (Actually, no statistically significant difference between these two quantities was observed). To get a quantitative estimate of the transition rate we measure the variance of  $N_{\text{CS}}$ , i.e.  $\delta^2 \equiv \langle N_{\text{CS}}^2 \rangle - \langle N_{\text{CS}}(t) \rangle^2$ , over an ensemble of 100 independent runs starting from different field configurations that have the same energy spectrum as shown in Fig. 3. The preparation of the initial configuration and other peculiarities of the numerical procedure will be discussed in detail in a future publication.

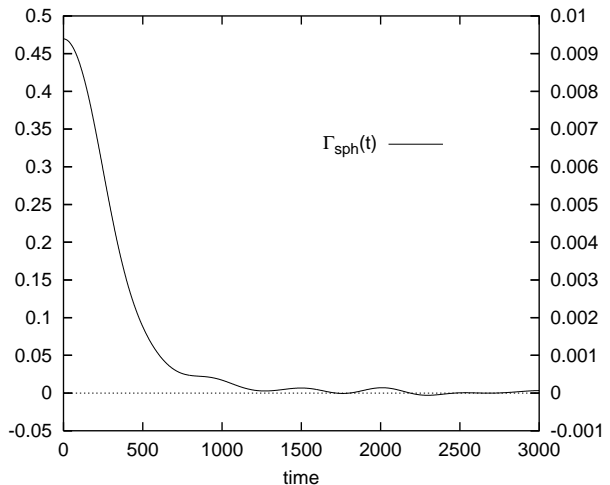


FIG. 13. The evolution of the sphaleron rate with time for the reduced-energy runs. The decrease of the final effective temperature in Fig. 12 results in the freezing out the equilibrium transitions soon after the resonance.

The variance of  $N_{\text{CS}}$  is shown in Fig. 6. Its time derivative  $d\delta^2/dt = \text{Volume} \times \Gamma_{\text{sph}}$  is plotted in Fig. 7. Note that this relation comes naturally from the diffusion of the Chern-Simons number,  $\langle N_{\text{CS}}^2 \rangle \simeq \text{Volume} \times \Gamma_{\text{sph}} t$ , which follows a typical Brownian motion [25]. Note that for initial parameters chosen as in Figs. 3-10, the rate actually increases during the thermalization of the Higgs field. However, for our purposes, it is important that we get a substantial amount of sphaleron transitions right after the beginning of the resonance. One could slow down the after-resonance transitions by decreasing the total energy of the system by a factor of 4 (see Figs. 11-15 below). However, this decreases the net generated asymmetry considerably, due to a decrease of the effective temperature  $T_{\text{eff}}$ , see Fig. 12, and the subsequent decrease in the sphaleron rate just after the resonance, see Fig. 13. These two sets of figures helps us gain intuition about the process of baryogenesis during preheating in (1+1) dimensions.

### B. The generation of the baryon asymmetry

As is clear from Eqs. (20) and (22), the chemical potential  $\mu_{\text{eff}} \propto -\kappa \partial_0 \langle \phi^* \phi \rangle$  is non-zero only during the resonance. The energy transfer from the inflaton to the Higgs field results in a steady shift of  $\langle \phi^* \phi \rangle$  expectation value, see Fig. 9. This shift in VEV acts as a chemical potential and drives the baryon asymmetry.

The baryon asymmetry generated by the non-equilibrium sphaleron transitions in the presence of a CP violating chemical potential  $\mu_{\text{eff}}$ , see Eq. (15), is observed as a non-zero value of  $\langle N_{\text{CS}} \rangle$  averaged over a computer-generated ensemble. As shown in Figs. 10 and 15,  $\langle N_{\text{CS}} \rangle$  steadily increases and eventually freezes when the expec-

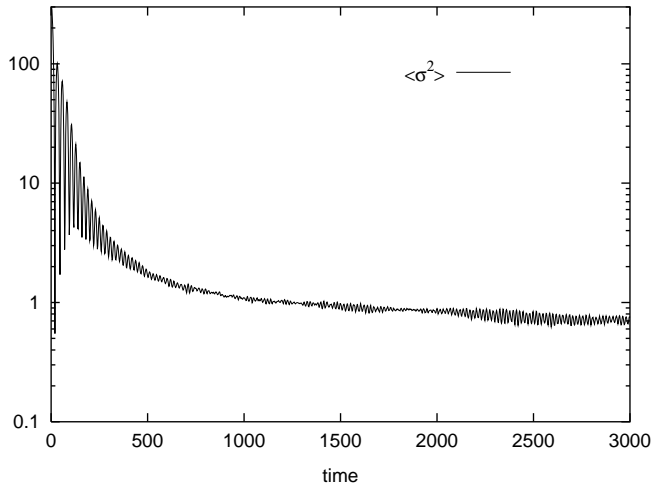


FIG. 14. The time evolution of  $\langle \sigma^2 \rangle$ , in units of  $v^2$ , for the reduced-energy runs of Figs. 11-13.

tation value  $\langle \phi^* \phi \rangle$  approaches a constant value and the chemical potential (15) vanishes. In the early universe, the drift of  $\langle N_{\text{CS}} \rangle$  is eventually interrupted by the decay of the vector and Higgs fields into fermions.<sup>4</sup> This leads to thermalization and, as long as the reheat temperature is sufficiently low, there is no further wash-out of the baryon asymmetry. We note in passing that, in our numerical simulations, the Chern-Simons number attained at the end (i.e. the final baryon number) is approximately linearly dependent on the CP violating parameter  $\kappa$ , and, therefore, our estimate can be extrapolated to very small values of  $\kappa$ .

## V. CONCLUSION

There is no empirical evidence that a thermal electroweak phase transition took place in the early universe. However, since the only well-established source of baryon number non-conservation is the gauge sector of the Standard Model, one could argue that electroweak baryogenesis [1] is the only explanation for the baryon asymmetry of the universe that does not invoke any unknown B-violating new physics. This reasoning would favor the usual electroweak phase transition, followed by the electroweak baryogenesis, on aesthetical grounds.

In this paper we have presented an appealing alternative. We have shown that a new kind of electroweak baryogenesis, which still uses only the known sources of baryon number violation, is possible even if the reheat

<sup>4</sup>The Higgs and vector decays into fermions are not included in our (1+1)-dimensional simulations. There has been recent progress [31] in introducing fermions in (1+1) lattice simulations, but we will leave for future work such developments.

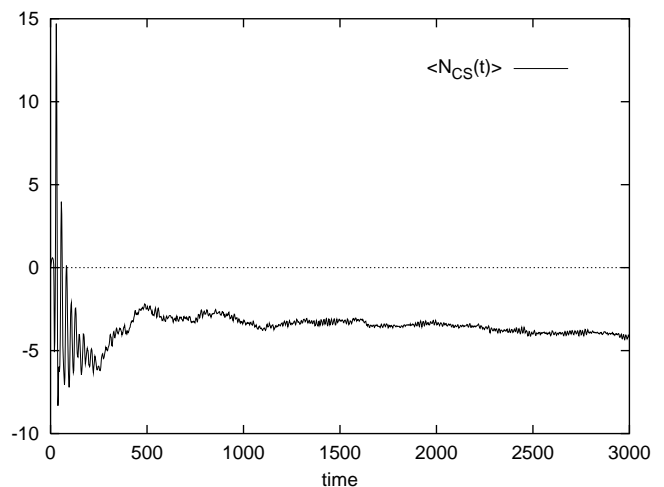
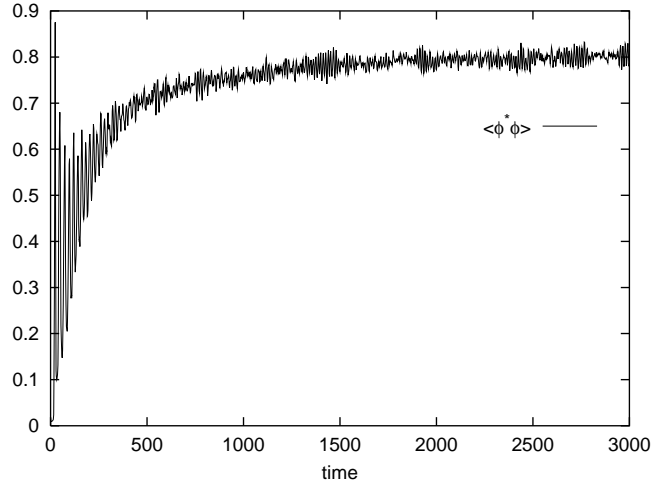


FIG. 15. The time evolution of  $\langle \phi^* \phi \rangle$ , in units of  $v^2$ , and  $\langle N_{\text{CS}}(t) \rangle$ , for the reduced-energy runs of Figs. 11-13.

temperature after inflation was too low for a thermal restoration of the  $\text{SU}(2) \times \text{U}(1)$  gauge symmetry. Moreover, the departure from thermal equilibrium, necessary for generating a non-zero baryon number density, is naturally achieved at preheating after an electroweak-scale inflation.

We discussed baryogenesis in the context of a new model of inflation that has several appealing features on its own. We assumed an economical extension of the (Supersymmetric) Standard Model with an inflaton field that is a singlet under the  $\text{SU}(3) \times \text{SU}(2) \times \text{U}(1)$  gauge group. We further assumed that there is a bi-quadratic coupling of the inflaton field to the standard Higgs doublet. The slow-roll motion of the inflaton triggers the spontaneous breaking of the electroweak symmetry, while the ordinary Higgs VEV ends inflation. The oscillations of the inflaton drive an explosive production of the Higgs modes with long wavelengths and large occupation numbers.

We have presented a novel scenario for baryogenesis.

It takes advantage of the dramatic departure from equilibrium at preheating that follows inflation. Sphaleron transitions take place during preheating, before the thermalization of the plasma. Baryon asymmetry can be generated through sphalerons in a manner similar to the usual electroweak baryogenesis [2]. When the universe reaches thermal equilibrium, the temperature can be small enough to suppress further baryon-violating processes, so that the baryon asymmetry is not washed out.

### ACKNOWLEDGEMENTS

J.G.B. thanks the organizers of the ITP workshop on *Non-equilibrium quantum fields*, Santa Barbara (January 1999), where this work was presented, for a very stimulating atmosphere, and the participants of the workshop for generous discussions. J.G.B. also thanks Belen Gavela and Andrei Linde for enlightening comments and suggestions. J.G.B. is supported by a Research Fellowship of the Royal Society of London. D.G. thanks D.V. Semikoz and M.M. Tsypin for stimulating discussions. D.G. is grateful to CERN TH division for kind hospitality. D.G. work was also supported in part by RBRF grant 98-02-17493a. A.K. thanks J.M. Cornwall for helpful discussions. The work of A.K. was supported in part by the US Department of energy grant DE-FG03-91ER40662. We thank Igor Tkachev for many valuable comments.

---

[1] V.A. Kuzmin, V.A. Rubakov, and M.E. Shaposhnikov, Phys. Lett. B155 (1985) 36.  
[2] For review, see V. A. Rubakov and M. E. Shaposhnikov, Phys. Usp. 39 (1996) 461.  
[3] A. D. Sakharov, JETP Lett. **6**, 24 (1967).  
[4] L. Kofman, A. Linde and A. A. Starobinsky, Phys. Rev. Lett. **73**, 3195 (1994); Phys. Rev. D **56**, 3258 (1997).  
[5] L. Kofman, A. Linde and A. A. Starobinsky, Phys. Rev. Lett. **76**, 1011 (1996); I.I. Tkachev, Phys. Lett. **B376**, 35 (1996).  
[6] E. W. Kolb, A. Linde and A. Riotto, Phys. Rev. Lett. **77**, 4290 (1996); G. W. Andreson, A. Linde and A. Riotto, Phys. Rev. Lett. **77**, 3716 (1996); E. W. Kolb, A. Riotto and I. I. Tkachev, Phys. Lett. B **423**, 348 (1998).  
[7] A.D. Linde, Phys. Lett. **B259**, 38 (1991); Phys. Rev. D **49**, 748 (1994).  
[8] A. D. Linde *Inflationary Cosmology and Particle Physics*, Harwood Academic Press, New York, 1990.  
[9] L. Knox and M. Turner, Phys. Rev. Lett. **70** (1993) 371.  
[10] L. Randall, M. Soljačić and A. H. Guth, Nucl. Phys. B **472**, 377 (1996); J. García-Bellido, A. D. Linde and D. Wands, Phys. Rev. D **54**, 6040 (1996).  
[11] G. Giudice and R. Rattazzi, Phys. Rep., in press, hep-ph/9801271 (1998).  
[12] C. L. Bennett et al., Astrophys. J. **464**, L1 (1996).

[13] J. R. Bond, in *Cosmology and Large Scale Structure*, Les Houches Summer School Course LX, ed. R. Schaeffer (Elsevier Science Press, Amsterdam, 1996).  
[14] J. García-Bellido and D. Wands, Phys. Rev. D **54**, 7181 (1996).  
[15] N. Kaloper and A. Linde, hep-th/9811141 (1998).  
[16] J. F. Gunion, H. E. Haber, G. Kane, and S. Dawson, *The Higgs Hunter's Guide*, Addison-Wesley, New York, 1996.  
[17] J. García-Bellido and A. D. Linde, Phys. Rev. D **57**, 6075 (1998).  
[18] S. Yu. Khlebnikov and I. I. Tkachev, Phys. Rev. Lett. **77**, 219 (1996); Phys. Rev. Lett. **79**, 1607 (1997).  
[19] T. Prokopec and T. G. Roos, Phys. Rev. D **55**, 3768 (1997).  
[20] A. A. Grib, S. G. Mamayev, and V. M. Mostepanenko, *Vacuum quantum effects in strong fields*, Friedmann Laboratory, St. Petersburg, 1994.  
[21] N. W. McLachlan, *Theory and application of Mathieu functions*, Oxford University Press, Oxford, 1951.  
[22] D. Yu. Grigoriev, V. A. Rubakov and M. E. Shaposhnikov, Phys. Lett. **B216**, 172 (1989); Nucl. Phys. **B326**, 737 (1989).  
[23] D. Bodeker, Phys. Lett. **B426**, 351 (1998).  
[24] P. Arnold, L. McLerran, Phys. Rev. D **36**, 581 (1987).  
[25] S. Yu. Khlebnikov, M. E. Shaposhnikov, Nucl. Phys. **B308**, 885 (1988).  
[26] P. Arnold, D. T. Son, and L. G. Yaffe, Phys. Rev. D **55**, 6264 (1997).  
[27] M. Shaposhnikov, Nucl. Phys. **B299**, 797 (1988).  
[28] D. Yu. Grigoriev, M. E. Shaposhnikov and N. G. Turok, Phys. Lett. **B275**, 395 (1992).  
[29] W.H. Tang and J. Smit, hep-lat/9805001 (1998).  
[30] D. Yu. Grigoriev, in: Procs. of the 10th Int. Seminar QUARKS-98.  
[31] G. Aart and J. Smit, hep-ph/9812413 (1998).